Ring Pseudorotation in Pyrrolidine *N*-Oxyl Radicals: an Analysis of ^{13}C-Hyperfine Structure of EPR spectra

Antal Rockenbauer,[*,a] **László Korecz**[a] **and Kálmán Hideg**[b]
[a] *Central Research Institute for Chemistry, Hungarian Academy of Sciences H-1525, Budapest, P.O. Box 17, Hungary*
[b] *Central Laboratory of Chemistry, University of Pécs, H-7643, Pécs, P.O. Box 99, Hungary*

^{13}C-Hyperfine parameters have been determined for 36 substituted pyrrolidine *N*-oxyl free radicals by computer simulation of the ^{13}C satellites in the EPR spectra. The β-carbon couplings were computed as an average value of twenty twist and envelope conformations weighted by the Boltzmann factors. The ring pseudorotation was described by a potential $V = 1/2V_1[1 - \cos(P - P_1)] + 1/2V_2[1 - \cos 2(P - P_2)]$, where P is the pseudorotational phase. The parameters of the potential function were adjusted in order to reproduce the measured β-carbon couplings and temperature coefficients. In the case of symmetrically substituted molecules the equilibrium conformation is the T_1 twist with a potential barrier 11.4 ± 2 kJ mol^{-1}. Substituents can deform the equilibrium conformation towards the E_3 envelope. The V_1 barrier characterising the equatorial–axial preference of substituents was found to be larger at the ring positions 3 and 4 than at 2 and 5. The effect of multisubstitution is described by a vector addition model of the pseudorotational potential, and examples are given for the assignment of *cis–trans* configurations. The axial–equatorial preferences of substituents were determined from the linewidth variation in the nitrogen triplet pattern. The 2-aryl and 2-ethynyl substituents revealed an axial preference indicating the existence of long-range conjugation between the π-systems of the NO moiety and the substituent. The substituent dependence of nitrogen hyperfine coupling is also explained in terms of the pseudorotational model.

Flexible five-membered rings represent the best examples of pseudo-rotation since in cyclopentane the competing endocyclic bending and torsional forces effectively cancel each other,[1] and thus the symmetric twist (half-chair) and envelope (bent) conformations possess nearly identical energies. Either endo-or exo-cyclic substitution can deform the smooth pseudorotational potential of cyclopentane by resolving the conformational degeneracies. The ring, however, keeps its high flexibility, that is a wide range of conformations—often the entire pseudorotational itinerary—remains thermally populated, and fast interconversion can occur between the populated conformers. Consequently, the concept of 'frozen conformations'—often successfully applied in the characterisation of six-membered ring geometries[2]—breaks down in the case of five-membered rings. A typical example is given by NMR spectroscopy when the ring puckering is predicted from the vicinal proton coupling constants,[3] or the difficulties in the use of gas-phase electron diffraction to derive ring geometry from the radial distribution of the diffraction pattern.[4] Whether the applied measuring technique is fast or slow compared with the rate of conformational interconversion, we have to use a different integration procedure to calculate the contributions of thermally populated conformations to the geometry-dependent spectroscopic or diffraction parameters. In the case of fast techniques, *e.g.*, the observed bands in the IR or Raman spectra[5] or the distributions in the ED technique[4] become diffused owing to the superimposed contributions of each conformation. On the other hand, for the 'slow' spectroscopic techniques, like EPR[6] or NMR,[3] the bands remain sharp and their positions are determined as a population-weighted average of individual band positions corresponding to the interconverting conformers. In the intermediate case, when the timescale of measurement is comparable to the rate of interconversion, 'dynamic' spectra can be recorded. NMR[7] and EPR[8] can easily be used when six-membered rings are studied, but for the case of five-membered rings only the low-temperature matrix technique is able to make the interconversion slow enough for the detection of dynamic EPR spectra.[9]

In the present work we make an effort to develop an alternative EPR method that is capable of deriving quantitative information about the pseudorotation of five-membered rings. We attempt to utilize the relative simplicity of EPR spectra, which—in contrast with the IR, MW, ED or NMR techniques—produces a readily analysable spectrum even if the ring is substituted in a highly complex manner. In particular, we investigate the very stable pyrrolidine *N*-oxyl (pyrno) derivatives, where the positions 2 and 5 are completely substituted, but additional substitutions can also occur at the positions 3 and 4. As for the *N*-oxyl-type spin-label compounds the low temperature conditions would produce broad anisotropic lines, we could not record dynamic spectra; instead, we limit ourselves to the temperature region 200–350 K, where molecular tumbling is fast enough to obtain well-resolved hyperfine structure. The lack of β-hydrogen in the 2,2,5,5-tetrasubstituted pyrno derivatives seems to impose severe limitations, since the dihedral dependence of β-proton hyperfine coupling (hfc) could offer the most straightforward geometric information,[6] but we point out in this paper that the β-carbon hfc derived from the ^{13}C hyperfine satellites by computer analysis[10] is highly informative.

We present the ^{13}C hfc parameters for 36 substituted pyrno radicals (see Table 1), where our reference compound **1** is 2,2,5,5-tetramethyl-pyrno. In order to determine the pseudorotational potential from these data, we first have to transcribe the Stone–Maki theory[11] originally developed to consider the effect of torsional motion on the β-proton hfc. With the help of transcribed model we have computed the pseudorotational potential barriers as well as the equilibrium geometry for the cases when the pyrno ring is differently substituted. The situation when a pair of *cis*- and *trans* isomers exists is analysed in detail. We also put forward the question of whether the axial–equatorial preference of substituents can be decided from EPR

Table 1 EPR spectroscopic data of pyrno radicals **1–36**

Compound	a_N/G	$(\Delta a_N/\Delta T)$/ mG deg^{-1}	l_2/l_3 (at −60 °C)	a_{C^α}/G [a]	a_{C^β}/G [b]	$(\Delta^a{}_{C^\beta}/\Delta T)$/mG deg^{-1} [c]
1	14.23	1.86	1.12	5.6	6.9 (4)	−1.1
2	14.23	1.36	1.14	5.2	9.2, 8.8, 5.4, 4.8	—
3	14.16	1.79	1.24	5.2	9.1 (2), 5.5 (2)	−2.7
4	14.20	2.00	1.28	5.4	9.5, 9.0, 5.7, 4.4	−2.5
5	13.78	1.57	1.36	5.6	6.4 (2), 6.0 (2)	−0.9
6	13.80	1.64	1.51	5.2	8.0 (2), 4.2 (2)	−3.8
7	13.91	1.64	1.41	5.2	8.7, 8.2, 5.6, 4.0	−3.6
8	13.88	1.21	1.31	5.5	8.8, 8.3, 4.5, 3.8	−2.6
9	14.45	2.20	1.43	5.8	9.5, 8.0, 6.8, 5.2	−3.6
10	14.22	1.80	1.53	6.0	9.0, 8.7, 5.0, 4.5	−2.5
11	14.45	2.20	1.59	5.6	9.7, 8.0, 6.5, 5.0	−5.0
12	14.21	1.80	1.74	5.8	9.0, 8.5, 4.5, 4.5	−2.1
13	14.20	1.90	1.15	5.6	7.2, 6.8, 6.5, 6.5	—
14	14.15	1.10	1.43	5.7	7.5, 7.0, 6.5, 6.5	−1.3
15	14.05	—	—	5.6	7.2, 6.8, 6.8, 6.5	—
16	13.88	—	—	5.7	11.0, 7.1, 6.1, 5.1	—
17	13.76	2.90	1.30	5.8	10.9, 7.0, 6.0, 5.0	−7.8
18	13.86	—	—	5.6	12.0, 7.0, 6.0, 5.0	—
19	14.35	1.67	1.48	4.7	13.0, 7.1, 5.6, 4.0	−4.0
20	14.20	—	—	5.3	6.8 (2), 6.3 (2)	—
21	14.09	—	—	5.7	8.0 (2), 5.9 (2)	—
22	14.15	—	—	5.7	7.2 (2), 6.4 (2)	—
23	13.98	—	—	5.6	7.9 (2), 6.2 (2)	—
24	14.13	—	1.44	5.7	7.2 (2), 6.0 (2)	—
25	14.00	—	1.60	5.8	8.0, 7.6, 6.2, 6.2	—
26	14.19	—	—	5.7	7.3 (2), 6.3 (2)	—
27	14.00	—	—	5.7	8.3, 7.9, 6.1, 6.1	—
28	13.95	1.0	1.20	5.8	7.0 (2), 6.3 (2)	−0.9
29	13.85	1.2	1.24	5.6	7.9 (2), 6.2 (2)	−5.8
30	14.16	1.0	1.51	5.8	6.8 (4)	−2.5
31	13.96	1.6	1.52	5.8	8.3 (2), 6.3 (2)	−2.2
32	13.70	1.4	1.55	5.9	10.6, 6.7, 6.2, 5.0	−7.6
33	13.76	1.9	1.38	6.0	11.0, 6.9, 6.5, 5.0	−5.2
34	13.22	2.0	2.32	5.7	10.8 (2), 4.8 (2)	−7.3
35	14.35	1.6	2.35	4.2	11.3 (2), 5.3 (2)	−1.4
36	14.40	1.5	1.94	4.2	12.6 (2), 4.6 (2)	−4.6

[a] Two equivalent carbons. [b] The number of carbons is given in parentheses. [c] Data are given for the largest carbon splitting.

data; for this purpose the usefulness of magnetic relaxation data is discussed. We also discuss the kind of information that can be gained from the ^{14}N hfc.

Theoretical

The hfc of the β-carbon is expected to show similar dihedral dependence to the β-hydrogens,[12] eqn. (1), where ρ_N is the

$$a_C = B_0\rho_N + B_2\rho_N\cos^2\theta, \qquad (1)$$

spin density on the p_z orbital of N, while θ is the dihedral angle between the planes $C_\beta C_\alpha N$ and $C_\alpha N$ p_z. Owing to the out-of-plane ring puckering vibration the dihedral angles of β-carbons in the 2,2,5,5-tetrasubstituted pyrno radicals will be time-dependent and a quantum-mechanical average of $\cos^2\theta$ should be calculated over the vibrational states of the ring [eqn. (2)].

$$\langle\cos^2\theta\rangle = \frac{\sum\limits_{i=0}^{\infty}\langle\cos^2\theta\rangle_i\exp(-E_i/kT)}{\sum\limits_{i=0}^{\infty}\exp(-E_i/kT)} \qquad (2)$$

The treatment is analogous with the case where the dihedral angle changes owing to hindered torsional motion,[11] but in our case the equation of motion should be solved for the out-of-plane puckering in the five-membered ring. Following the classification of Gwinn *et al.*,[13] the 'case 3', *i.e.*, the condition of a hindered pseudorotation holds true for the pyrno rings, in other words, the radial mode (oscillations of the pseudorotational amplitude) and the angular mode (hindered rotation or 'torsion' of P pseudorotational angle) can be separated. From the P angle the φ_j torsional angles of the ring atoms $j+1, j+2, j+3, j+4$ can be given by eqn. (3)[14] where φ_0 is the puckering

$$\varphi_j = \varphi_0\cos[P + 144(j-1)] \qquad (3)$$

amplitude. The above definition gives the T_1 (C_2) twist at $P = 0$ and 180, the E_1 (C_s) envelope at $P = 90$ and 270. The other T_j and E_j conformers are obtained if $P_j = 18(2j-2)$ and $P_j = 18(2j+3)$, respectively. The dihedral angles of β-carbons can be given by the φ_4 ($C_5NC_2C_3$) (Fig. 1) and φ_3 ($C_4C_5NC_2$) torsional angles; eqns. (4) and (5), where eqn. (4) gives the

$$\theta_{2,\beta} = 30 \pm \varphi_4, \rho_{5,\beta} = 30 \mp \varphi_3 \qquad (4)$$

$$\theta_3 = 90 - \varphi_4, \theta_4 = 90 - \varphi_3 \qquad (5)$$

dihedral angles of the β-carbons in the 2,2,5,5-substituents, while eqn. (5) stands for the ring C-3 and C-4 carbon atoms. Since the latter dihedral angles are rather large, the respective carbon hfc is small and non-detectable.

Though the dihedral angles depend both on φ_0 and P, the amplitude dependence is less sensitive and we will substitute the averaging over this coordinate by using its equilibrium value,

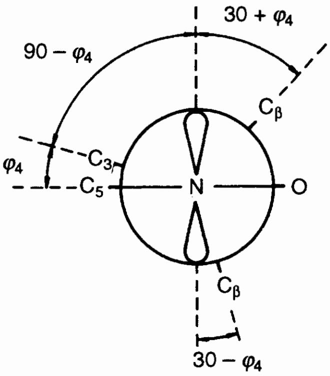

Fig. 1 The NC_2 Newman projection representing the relationship between dihedral angles $C_\beta C_2 Np_z$ and torsional angle $C_5NC_2C_3$

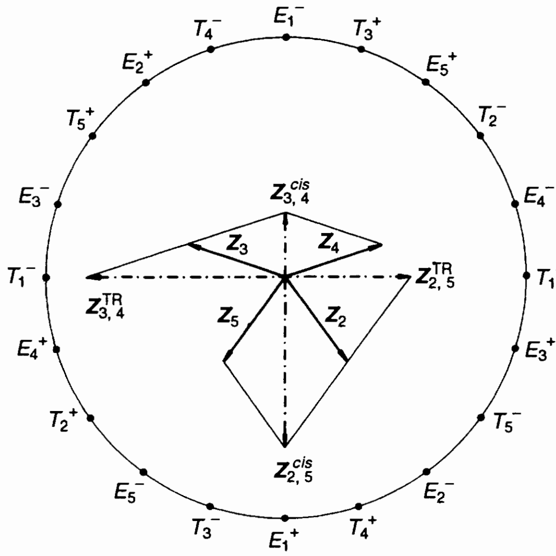

Fig. 2 Pseudorotational potential vectors representing the contribution of the *i*th exocyclic ring substituent to the term $\frac{1}{2}V_1[1-\cos(P-P_1)]$. There are identical substituents on positions 2,5 or 3,4, respectively, and all substituents have equatorial preference. The *cis* configuration is given as a sum, while the *trans* is given as a vector difference. The twenty symmetric twist and envelope conformations are shown as a function of pseudorotational phase.

and only the effect of pseudorotational angle will be considered. In the case of C_{2v} symmetry the equation of motion can be written as shown in eqn. (6).

$$\mathcal{H}(P) = -B\partial^2/\partial P^2 + \tfrac{1}{2}V_2(1-\cos 2P) + \tfrac{1}{2}V_4(1-\cos 4P) + \ldots \quad (6)$$

The expected order of magnitude of the parameters in eqn. (6) can be taken from the case of cyclopentanone, where the torsional and bond-bending strains are similar to our case. Far-IR spectroscopy,[15] *e.g.*, suggests a value of 15–20 kJ mol^{-1} for the V_2 barrier, while V_4 was found to be less than 1 kJ mol^{-1}. Thus the latter term can alter only slightly the thermal population and can be neglected in the averaging procedure of eqn. (2). The B rotational parameter is around 20 J mol^{-1} for cyclopentanone, and this value is further reduced due to the 2,2,5,5-substitution of the pyrno ring, thus the energy levels of eqn. (6) lie rather close and the quantum-mechanical averaging in eqn. (2) can be replaced by a classical integration[16] over the P pseudorotational angle. As a matter of convenience, we approximate this integral by a summation over the 20 symmetric C_2 twist and C_s envelope conformations, eqn. (7).

$$\langle\cos^2\theta\rangle = \frac{\sum_{i=1}^{20}\cos^2\theta_i\exp(-V_i/kT)}{\sum_{i=1}^{20}\exp(V_i/kT)} \quad (7)$$

When the pyrno ring contains different substituents at positions 2,3,4 and 5, the original molecular symmetry is distorted, and consequently, the $V(P)$ potential function deviates from the expansion in eqn. (6). We describe this distortion by including a term periodic within 360°, and furthermore we let the phase of the terms deviate from zero, eqn. (8). Here V_1

$$V(P) = \tfrac{1}{2}V_1[1-\cos(P-P_1)] + \tfrac{1}{2}V_2[1-\cos 2(P-P_2)] \quad (8)$$

characterises the energy difference of substituents if they have equatorial or axial positions. Supposing this energy preference originates from the non-bonded steric interactions,[17] the largest axial–equatorial energy preference is expected in the E_2, E_3, E_4 or E_5 conformations if the substitution is at the positions 2, 3, 4 or 5, respectively. This means that $P_1 = -54$ and 54 for the 2- or 5-substitution, while $P_1 = -18$ or 18 for the 3- or 4-substitution. Double substitution can be described in a straightforward way if we introduce a $\boldsymbol{Z}_1$ vector with polar coordinates (V_1, P_1). Then the combined effect of substituent vectors $\boldsymbol{Z}_1'$ and $\boldsymbol{Z}_1''$ can be given by the vector addition rule, eqn. (9).

$$\boldsymbol{Z}_1^{cis} = \boldsymbol{Z}_1' + \boldsymbol{Z}_1'' \text{ and } \boldsymbol{Z}_1^{trans} = \boldsymbol{Z}^{1'} - \boldsymbol{Z}_1'' \quad (9)$$

For identical substituents the *trans* configuration will produce a resultant vector with $P_1 = 0$ or 180, while in case of the *cis*-configuration $P_1 = 90$ or 270. For non-identical substituents a more complex situation occurs that does not obey any symmetry considerations. (See Fig. 2). Analogously, the substituent effect on the V_2 term can also be described by polar vectors. Here we must bear in mind that the vector addition rule is valid only if no further terms appear in the potential of eqn. (8).

Results and Discussions

The assignment of α-^{13}C *hyperfine couplings.*—The computer simulation technique described in detail in our earlier paper[10] permits the determination of six ^{13}C satellites: two α-carbons and four β-carbons* (the substituents of C-2 and C-5), while the C-3 and C-4 ring carbons give insufficiently large splittings which are hidden under the main ^{12}C line (Fig. 3). The precision of ^{13}C hfc is 0.1 G and two carbon bands can be distinguished only if their separation exceeds 0.5 G. The larger coupling can always be determined with high precision, therefore we give only the temperature coefficient for this coupling (Table 1). Unlike the ^{13}C NMR, the EPR spectra did not permit the determination of the sign of the coupling, thus the distinction of α- and β-carbon bands could be made only from the intensities of the bands. For compound **1** the four β-carbons are equivalent, thus the band of the intensity of four carbons with the hfc 6.9 G can be assigned to the β-carbons, while the other band of the intensity of two carbons with the hfc 5.6 G can be assigned to the α-carbons. As a consequence of ring substitution, the β-carbon band splits into two bands if two identical *cis*- or *trans*-substituents are present, and into four bands in the case of non-symmetrical substitution (see Fig. 4). No splitting was

---

* We follow the usual notation of EPR literature by using α and β to denote the carbons separated by one, or two sigma bonds from the π-odd electron centre.

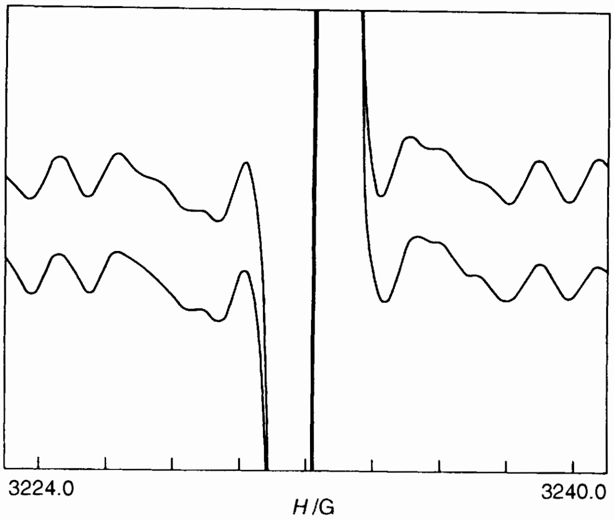

Fig. 3 Experimental (bottom) and simulated (top) ^{13}C-satellites of the central ^{14}N line in the EPR spectrum of radical **19**

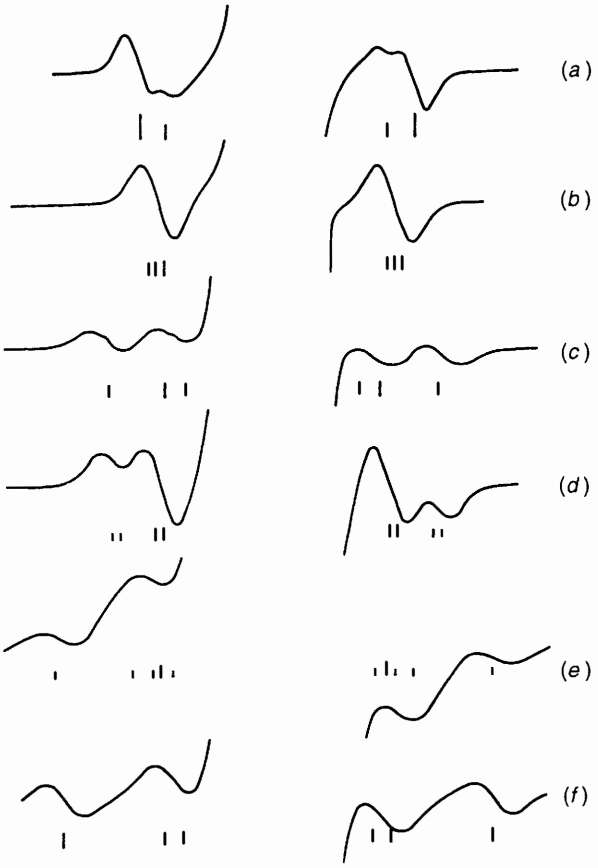

Fig. 4 The ^{13}C-satellites of the central ^{14}N line in the EPR spectra of **1** (*a*), **5** (*b*), **6** (*c*), **27** (*d*), **16** (*e*) and **34** (*f*) radicals; the stick diagram shows the positions of the satellites

observed for the α-carbon band and its position is remarkably invariant to the variation of substituents. For this reason we can assign the band of the two-carbon intensity with the hfc 5.6 ± 0.4 G to the α-carbons. There is, however, one notable exception, when ethynyl groups are present at position 2 or 5. In the case of 2-ethynyl substitution the only band having the intensity of two carbons is shifted to hfc 4.7 G, while for the 2,5-diethynyl molecules the only band that has the same position for both the *cis*- and *trans*-configuration is shifted to hfc 4.2 G. This means the ethynyl substitution can produce a significant decrease in α-carbon coupling.

β-Carbon Couplings and Pseudorotation Potential Parameters.—The parameters of pseudorotational potential in eqn. (8) can be adjusted in order to reproduce the β-carbon hfcs and temperature coefficients in Table 2. In this procedure we compare the experimental value of $\langle\cos^2\theta\rangle$ derived from the hfc data *via* eqn. (1) with the calculated value of $\langle\cos^2\theta\rangle$ given by the conformational average of eqn. (7), where the Boltzmann factors are determined by the potential function (8). The values of the adjusted parameters depend on the choice of $\rho_N B_0$ and $\rho_N B_2$ in eqn. (1). In our previous work where various cyclic *N*-oxyl radicals were studied,[10] the above parameters were found to be in the ranges (−1 to −2.2) and (11 to 13) G, respectively. Accordingly we adopt the parameters given in eqn. (10), and we

$$\rho_N B_0 = -1.5 \pm \text{G and } \rho_N B_2 = 12 \pm 1\text{ G} \qquad (10)$$

will also determine the confidence intervals of the adjusted parameters due to the error brackets in eqn. (10). In the cases of 2,5-ethynyl or aryl substitution the observed large β-carbon hfc and temperature coefficient could not be reproduced by the above choice of parameter; the adjustment needed larger parameter values such as those in eqn. (11). In the same

$$\rho_N B_0 = -3.4\text{ G} \pm 1\text{ G and } \rho_N B_2 = 17.7 \pm 1\text{ G} \qquad (11)$$

molecules the carbon splittings of a methyl or other alkyl group geminal to the ethynyl or aryl substituents can be interpreted in terms of slightly reduced hyperconjugation, eqn. (12).

$$\rho_N B_0 = -1.5 \pm 1\text{ G and } \rho_N B_2 = 10.5 \pm 1\text{ G} \qquad (12)$$

An additional fixed parameter in the adjustment procedure is the φ_0 puckering amplitude. From X-ray diffraction data[18] the puckering amplitude can be derived by means of eqn. (3). Its value varies between 36 and 42 (see Table 3) and the pseudorotational angle is close to $P = 0$, *i.e.*, the geometry in the solid phase is a slightly deformed T_1 twist conformation. Supposing that the puckering amplitude does not differ strongly in the liquid and solid phase, we adopted $\varphi_0 = 42$. An error range of ± 3 was found to alter only slightly the adjusted V_1 and V_2 values.

For compound **1** the β-carbon coupling (6.9 G) is larger than the free rotational average (4.5 G) and the temperature coefficient is negative, which suggests a preferential T_1 twist geometry with the P_0 equilibrium phase of 0 and 180. Owing to the C_{2v} symmetry, $V_1 = 0$ and the adjustment gives a potential barrier $V_2 = 11.4$ kJ mol^{-1} (see Table 2). This means the 2,2,5,5-tetramethylpyrno **1** indeed shows a hindered pseudorotation similar to the cyclopentanone ring, though the potential barrier is somewhat lower in the pyrno ring. It seems, however, the cyclopentyl radical represents an even closer analogy to pyrno, where not only the geometry of ground-state conformation (T_1), but also the free-energy difference ($\Delta G = 11.7$ kJ mol^{-1}) is the same.[9b]

Substitution at Position 3.—Additional substitution of pyrno at position 3 (compounds **2–4**) reduces the molecular symmetry and leads to the appearance of term V_1 in the potential function. We fixed $P_1 = 18$ and adjusted the barriers V_1 and V_2. The computations gave a rather large V_1 equatorial–axial preference ($V_1 = 10$ kJ mol^{-1}) and V_2 was also increased (see Table 2). The latter fact indicates stronger torsional energy due to the extra substitution that favours the twist conformation over the envelope one. The equilibrium geometry is no longer the symmetric C_2, but is distorted slightly towards the neighbouring E_3 ($P = 18$) conformer. The distortion is rather small ($P_0 = 3$) and seems not to be sensitive to the type of substituent at the position 3. This fact permits comparison of the

Table 2 Adjusted pseudorotational potential parameters of pyrno radicals

Compound	Substitution	V_1/kJ mol^{-1}	P_1/deg	V_2/kJ mol^{-1}	P_2/deg	P_0/deg
1	—	0[a]	—	11.4(2)[b]	0[a]	0
2, 3, 4	3-	10(1)[b]	18[a]	14(2)	1(1)	3(1)
5	*cis*-3,4-	2(0.5)	90[a]	15(2)	0[a]	2(0.5)
6	*trans*-3,4-	7.9(1)	0[a]	12(3)	0[a]	0
7	*cis*-3,4-	10(1)	14(4)	14(2)	1(1)	2.5(1)
8	*trans*-3,4-	8(1)	20(2)	14(2)	1(1)	2.5(1)
9, 11	*cis*-3,4-	8(1)	54(4)	13(1)	3(1)	9.5(1)
10, 12	*trans*-3,4-	14(4)	5(3)	11(4)	3(1)	3.5(1)
13, 14, 15	2-	1.5(0.5)	54[a]	11(2)	0[a]	1.5(0.5)
16, 17, 18	2-	5(1)	54[a]	11(2)	3(1)	8(1)
19	2-	13(1)	40(20)	11(2)	1(1)	9(2)
20, 22, 24, 26, 28, 30	*cis*-2,5-	2(0.5)	90[a]	11(2)	0[a]	2.5(0.5)
21, 23, 25, 27, 29, 31	*trans*-2,5-	3.5(0.5)	0[a]	9(3)	0[a]	0
32	*cis*-2,5-	4(1)	40(10)	11(2)	4(1)	5.5(1)
33	*trans*-2,5-	5(1)	80(5)	11(2)	4(1)	10(1)
35	*cis*-2,5-	11(1)	90[a]	11(2)	2(2)	16(2)
36	*trans*-2,5-	9(1)	0[a]	11(2)	0[a]	0
34	*trans*-2,5-	5(1)	0[a]	11(2)	0[a]	0

[a] Fixed parameters. [b] The errors are given in parentheses.

Table 3 Puckering parameters and space group of pyrno radicals

R^3	R^4	φ_0/deg	P_0/deg	Z	Space group	Ref.
COOH	—	39	8	4	$P2_12_12_1$	18(*a*)
$CONH_2$[a]	—	40	10	8	$P2_1/c$	18(*b*)
$CONH_2$[b]	—	36.4	−2	8	$P2_1/c$	18(*b*)
$CONH_2$	—	40.8	3.3	2	$P2_1$	18 (*b*)
CH_2OH	—	38.2	4	2	$P2_1$	18 (*c*)
OH	—	36.8	10	4	$P2_12_12_1$	18(*d*)
CN	CN[c]	42	13	8	*Pbcn*	18(*e*)

[a] Raceme (A). [b] Raceme (B). [c] *trans*.

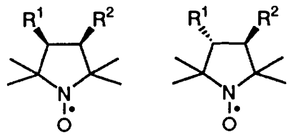

(*Z*) (*E*)

No.	R^1	R^2
1	H	H
2	CH_2OH	H
3	CH_2Br	H
4	Ph	H
5 (*Z*)	CN	CN
6 (*E*)	CN	CN
7 (*Z*)	CH_2NO_2	CN
8 (*E*)	CH_2NO_2	CN
9 (*Z*)	Ph	CO_2Me
10 (*E*)	Ph	CO_2Me
11 (*Z*)	Ph	COPh
12 (*E*)	Ph	COPh

equilibrium geometry in the liquid state with that in the solid. There are a few pyrno derivatives, in which the crystal geometry is available from X-ray diffraction studies[18] (Table 3). Table 3 shows identical pseudorotational phase angles in both solid and liquid for the optically active 3-carbamide and 3-hydroxymethyl derivatives, but the solid geometry is significantly shifted towards E_3 for the hydroxy-, carboxy- and one of the racemic carbamide derivatives ($P_0 = 8$–10), while a distortion towards the E_4 geometry occurs ($P_0 = -2$) for the other racemic carbamide derivative. The deviations of solid- and liquid-state geometries may be accounted for by the different strength of hydrogen bonds between neighbouring molecules. If the crystal point group is $P2_1$ and only two molecules are in the unit cell ($Z = 2$), hydrogen bonds occur only between the translationally shifted molecules and the respective O···H bonds are rather long (*ca.* 3.1 Å). In this case the solid- and liquid-state geometry was found to be identical. For the space groups, where $Z = 4$ or 8, a complex network of hydrogen bonds can be formed with much shorter O··· H distances (2.6–2.8 Å), which may explain the deviation of the ring geometries in the solid and liquid phases.

Substitution at Positions 3 *and* 4.—If positions 3 and 4 are substituted by identical groups (**5**, **6**), the C_s symmetry fixes $P_1 = 90$ for the *cis*- and the C_2 symmetry fixes $P_1 = 0$ for the *trans*-configuration. On carying out the V_1 *adjustment for the above case we obtained a much smaller* V_1 barrier to the *cis*- than to the *trans*-configuration. This fact is in accordance of the vector addition rules in eqn. (9), if $P_1 = 18$ and $P_1'' = -18$ for the 3- and 4-substituents, respectively.

For unlike substituents (compounds **7**–**12**) the distinction between *cis*- and *trans*-configurations is not so clear cut. Even so, for any $\mathbf{Z}_1'$ and $\mathbf{Z}_2''$ substituent vectors, the resulting $\mathbf{Z}_1$ vector should be larger for the *trans* than for the *cis*-configuration, furthermore, the resulting P^1 and P_0 phase angles should be smaller for the *trans* case. This holds true whether the C-3 atom is substituted by a phenyl and C-4 by a COOMe or COPh group (compounds **9**–**12**). However the opposite situation occurs if cyanide and nitromethyl substituents are present (**7** and **8**). This contradiction can be resolved if we assume the opposite conformational preference for the CN and nitro-methyl groups: while the former prefers the equatorial, the latter prefers the axial position, probably due to the dipolar interaction between the nitro and aminoxyl groups.[19] This conclusion is later supported by the analysis of magnetic relaxation data.

Replacement of the 2-*Methyl Group*.—If we replace one of the 2,2-methyl groups of **1** by an alkyl group (compounds **13**–**15**), the β-carbon bands reveal only a small separation. This observation is parallel with the findings of Zhang[20] who claimed the 4-substitution of the pyrno ring produces a much larger non-equivalence of β-protons than does 2-substitution. By assuming $P_1 = 54$ the V_1 adjustment leads to a rather small value (Table 2). On the other hand, the adjusted V_1 values are rather large for 2-aryl and 2-ethynyl substitutents (compounds

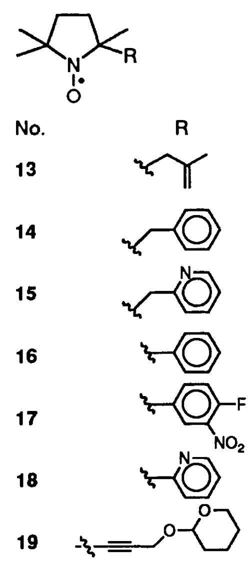

16–19) and the equilibrium geometry is *ca.* halfway between the T_1 and E_3 conformers (see Table 2). In this case the enhanced $\rho_N B_2$ value suggests an additional spin-transfer mechanism in addition to hyperconjugation. We presume a direct π-interaction can occur between the NO and aryl or ethynyl groups.[21] In this case the highest overlap of π-systems is expected when the dihedral angle of RC_2N and C_2N_z planes is zero. The adjusted P_1 value confirms this assumption, since when $P_1 \approx 40$, the dihedral angle is approximately zero for the pseudoaxial position. This observation also indicates the pseudoaxial orientation of 2-aryl and 2-ethynyl groups.

Replacement of 2- *and* 5-*Methyl Groups*.—If one methyl group of **1** is replaced both at the positions 2 and 5 by other alkyl groups (compounds **20–31**), the separation of the β-carbon bands and the adjusted V_1 barriers are similarly small (Table 2). In spite of this fact, the separation of the β-carbons for the *trans*-configuration is large enough to offer a straightforward way of distinguishing it from the *cis*-configuration. In the 2-aryl, 5-alkyl derivatives **32** and **33** only one of the β-carbons has a large hfc and temperature coefficient. The adjustment procedure gives larger P_1 and P_0 values for the *trans*- than the *cis*-configuration, which shows, according to the vector addition rule [eqn. (9)] that the aryl group should have the opposite conformational preference than that of the alkyl groups. Consequently, while the alkyl group is pseudoequatorial, the aryl group can assume a pseudoaxial orientation.

In the case of 2,5-diaryl substitution only one configuration could be synthesized (compound **34**). The adjustment procedure led to reasonable parameters only when P_1 was zero, that is, the configuration should be *trans* in this case. For the *cis*- and *trans*-2,5-diethynyl derivatives **35** and **36**, the well resolved β-carbon bands reveal only a slight difference, but the temperature coefficient is large only for the *trans*-configuration. Assuming $P_1 = 0$ and 90 for the *trans*- and *cis*-configuration, respectively, we obtained V_1 values that are less than the barrier obtained for the 2-ethynyl derivative **19**. This fact clearly contravenes the vector addition rule [eqn. (9)], that is the simple potential function given by eqn. (8) did not describe well the pseudorotation. A more reliable potential function is expected if it is periodic, not with the P phase, but with the dihedral angle θ. For the *trans*-configuration such a model yields a double-minimum curve with wells at *ca.* $P = 30$ and -30 and a local maximum at $P = 0$. The existence of a local maximum at $P = 0$ is supported by the reduced α-carbon constant observed for the radicals with 2- and 5- ethynyl substituents. As we established earlier,[10] the reduced α-carbon coupling is indicative of a C(C)NO pyramidal distortion. Such a distortion, however, could not occur if the ground conformation is the T_1 twist due to the C_2 symmetry. Pyramidal distortion is expected, however, if there is a rapid interconversion between conformers T_2 and T_5 ($P = 36$ and -36) or E_4 and E_3 ($P = 18$ and -18). For the *cis*-configuration the adjustment procedure suggests a strong deviation from C_2 symmetry ($P_0 = 16$), that is, the equilibrium conformation essentially agrees with the E_3 envelope geometry. This structure is again compatible with the small value of the α-carbon hfc.

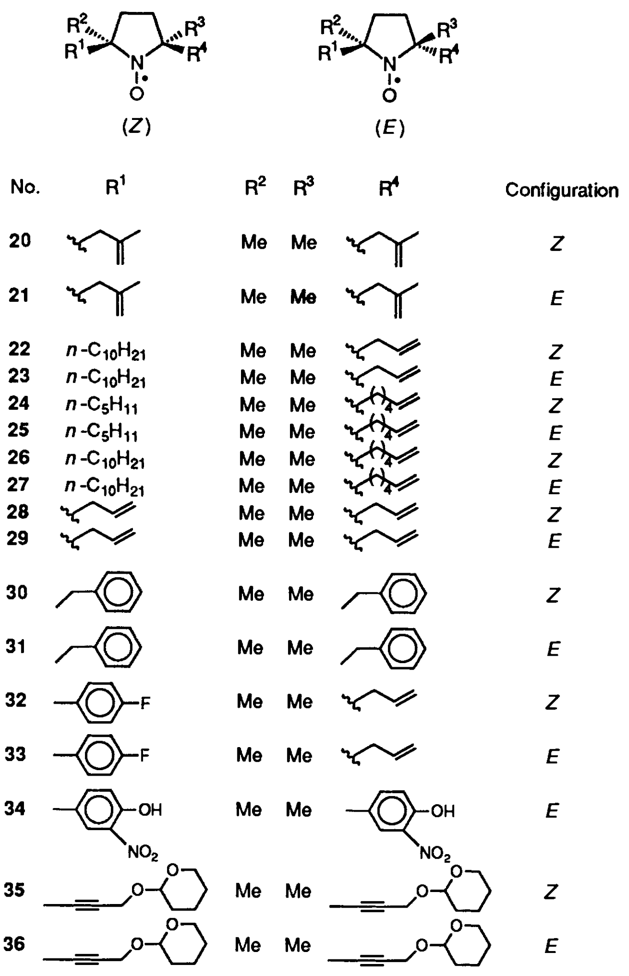

^{14}N *Hyperfine Coupling*.—The ^{14}N hfc for the pyrno radicals is small and reveals a positive temperature coefficient in a contrast with the data for the piperidine *N*-oxyl radicals.[10] The small a_N value is in accordance with the equilibrium conformation T_1, since then no C(C)NO pyramidal distortion can occur, which may give a substantial contribution to the nitrogen hfc. Owing to the small V_2 barrier the other conformations are also thermally populated, which explains the positive temperature coefficient. In order to estimate the a_N contributions of conformations, we assume a P phase dependence in the form of eqn. (13) where $a_N(0)$ is the nitrogen coupling in the T_1

$$a_N = a_N(0) + \Delta a_N \sin^2 P \qquad (13)$$

equilibrium conformation with symmetry C_2, while a_N has a maximum value in the conformation E_1, where the C_s symmetry allows a significant pyramidal distortion for the C(C)NO group. Owing to the rapid pseudorotational motion an average value of $\sin^2 P$ should be calculated, which can be carried out by the classical approximation of eqn. (7). For compound **1** the a_N

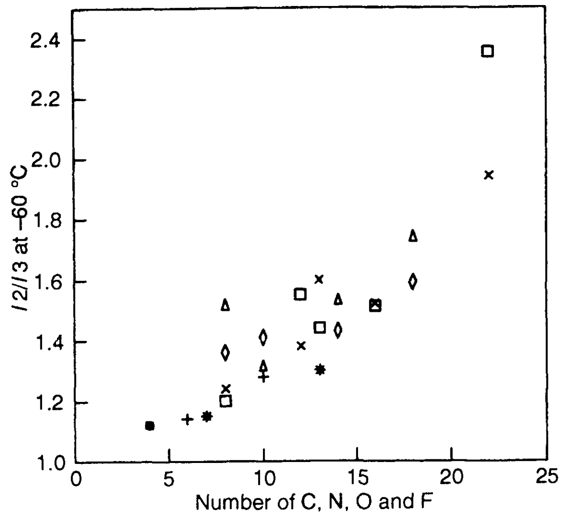

Fig. 5 The I_2/I_3 amplitude ratio of nitrogen triplet for pyrno radicals at -60 °C. The reference compound **1** is indicated by ■, the mono 3-, mono 2-, *cis*-2,5-, *trans*-2,5-, *cis*-3,4- and *trans*-3,4-substituents are indicated by symbols +, *, □, ×, ◇, and △, respectively.

value and its temperature coefficient can be reproduced by the values given in eqn. (14) where in the adjustment procedure we

$$a_N(0) = 13.8\ \mathrm{G} \text{ and } \Delta a_N = 3.5\ \mathrm{G}, \qquad (14)$$

used the rotational barrier $V_2 = 11.4$ kJ mol^{-1} obtained from the analysis of the β-carbon hfc.

Eqn. 13 can also explain why the *cis*-configuration gives an a_N value typically larger by 0.2 G than that of the *trans*-configuration (see Table 1): in the former case $P_1 = 90$, and consequently, one of the two E_1 envelope conformations becomes thermally more accessible. Assuming identical V_1 for the *cis*- and *trans*-configurations a barrier of $V_1 = 7$ kJ mol^{-1} may explain the observed 0.2 G difference of nitrogen couplings. Naturally, if V_1 is small for the *cis*-configuration, *cf* the case of the 3,4-dicyano derivative **5**, then no difference is obtained for a_N in the *cis*- and *trans*-configuration.

In Table 1 some anomalies can be seen in the a_N values of 2,5-aryl and -ethynyl derivatives (compounds **19**, **32**–**36**). In the former case a_N is reduced by 0.4 G if one, and by 0.9 G if two aryl substituents are present. This reduction can be explained by a small percentage decrease in ρ_N spin density, that is, increased spin density on the aryl carbon is accompanied by a reduction in spin density on the nitrogen. The 2- and 5-ethynyl substitution leads to a more complex situation, since then a significant C(C)NO pyramidal distortion occurs that not only reduces the α-carbon coupling, but simultaneously increases the a_N value. We observed such a trend in our earlier paper:[10] owing to the pyramidal distortion the increase in a_N and the decrease in the α-carbon hfc is about the same. By considering this contribution we would expect $a_N = 15.0$ G for 2-ethynylpyrno **19**, and $a_N = 15.6$ G for the 2,5-diethynyl compounds **35** and **36**. The actual measured a_N values are smaller by 0.7 G in the former, and by 1.2 G in the latter case. This again shows that the spin density transfer to the ethynyl group is accompanied by a reduction in spin density on the nitrogen.

Relaxation Times and Conformational Preferences.—For the investigated pyrno derivatives there is only a small difference in the magnetic anisotropies of the g and a_N tensors, thus the relaxation times of the nitrogen triplet lines depend almost exclusively on the rate of rotational tumbling of the molecules. A simple parameter that characterises quite well the relaxational rates is the amplitude ratio of the second and third lines of nitrogen triplet, eqn. (15). If the molecular rotation is fast then

$$r = I_2/I_3 \qquad (15)$$

r is close to unity, if the rotation is slow the r value increases. The rotational rate depends on the moment of inertia tensor of the molecules and the temperature and viscosity of medium. If the latter factors are identical (we always used toluene solutions and measured r at -60 °C, see Table 1), we can compare the moment of inertia of the differently substituted molecules.

In Fig. 5 we plotted r as a function of the number of C, N, O and F atoms in the 2-, 3-, 4-, and 5-subtitutents. As expected r increased with this number. More important, however, is that we can gain information about the axial–equatorial preferences if we compare the r value for the *cis–trans* pairs. Either for flexible or for rigid but symmetric substituents the equatorial position supposedly increases the moment of inertia to a larger extent than does the axial position (if the substituent itself has a bending conformation due to a hindered internal torsion, then the overall moment of inertia of the molecule may exhibit more complex behaviour, see, *e.g.*, **30** and **31**). In the case of doubly substituted molecules we can expect $r_{ee} > r_{ae} > r_{aa}$ where the a and e subscripts refer to the axial or equatorial positition of substituents. Owing to the twist geometry of pyrno ring , the *trans* configuration can have two equatorial substituents in the case of equatorial preference $r_{trans} = r_{ee}$ or two axial substituents if this orientation is preferred by the substituents $r_{trans} = r_{aa}$, while the *cis*-configuration always has one equatorial and one axial substituent $r_{cis} = r_{ae}$.

The order of r_{cis} and t_{trans} offers a straightforward way of deciding the axial–equatorial preference. If $r_{trans} > r_{cis}$ there is an equatorial preference. If, however, $r_{cis} > r_{trans}$ the substituents favour the axial position.

Fig. 5 shows that $r_{trans} > r_{cis}$ holds true for the *cis–trans* pairs when alkyl substitution occurs either at the 3,4 or at the 2,5 positions, and also in the cases when CN, COOMe or COPh groups are at positions 3 and 4. This means the above substituents prefer the equatorial orientation. On the other hand, $r_{cis} > r_{trans}$ is valid for the *cis–trans* pair **7**, **8** indicating the nitromethyl group should have an axial preference in agreement with the above assignment based on the separation of β-carbon splittings. The rather small value of r_{trans} for **8** indicates a compact geometry, which may be formed if the nitromethyl group is bent towards the NO group. For the diethynyl pair **35**–**36**, and for the mixed aryl–alkyl pair **32**–**33** $r_{cis} > r_{trans}$ holds true, which shows the axial preference of 2-ethynyl and 2-aryl groups, supporting the above findings obtained from the analysis of the β-carbon hfc.

Conclusions

In this paper we give ample evidence that the analysis of ^{13}C-satellites in the EPR spectra of pyrno radicals can offer a wealth of information about the pseudorotation of the five-membered ring. The height of the potential barrier and the equilibrium phase of pseudorotation can be obtained with at least the same accuracy as with other spectroscopic techniques such as MW or IR. Our method is particularly useful if a complicated pattern of substituents exists, since, even in this case, a reliable pseudorotational potential function can be gained. It is also possible to determine the equatorial–axial preference of substituents, and in most of the cases, straightforward assignments of the configuration of the *cis–trans* isomers can be made which obviates the tedious chemistry of the Mosher synthesis[22] or isotope enrichment of ^{13}C carbons.

Experimental

Compounds.—Pyrno radicals **1**,[23] **2**–**4**,[24] **5**–**6**,[18e] **7**–**8**,[25] **9**–

12,[26] **13–15**,[27] **16**,[26] **17**,[28] **18–25**,[27] **26–31**,[29] **32–33**,[27] **34**[28] and **35–36**[27] were prepared as described in the references.

Spectra.—The spectra were recorded with a JEOL type JES-FE-3X spectrometer in the X-band mode with 100 Hz field modulation. Degassed toluene solutions of concentration 10^{-4} mol dm^{-3} were used and the temperature of the measurements was varied between 200 and 350 K. The spectra after digitalisation were computer-simulated by a procedure given earlier.[10]

Acknowledgements

This work was sponsored by grants of the National Research Fund, Hungary: OTKA 1792/89 and 42/3 and by the Ministry of Welfare, Hungary: T575/1990.

References

1 K. S. Pitzer and W. E. Donath, *J. Am. Chem. Soc.*, 1959, **81**, 3213.
2 C. Romers, C. Altona, H. R. Buys and E. Havinga, *Top. Stereochem.*, 1969, **4**, 39.
3 B. Fuchs, *Top Stereochem.*, 1978, **10**, 1.
4 A. C. Legon, *Chem. Rev.*, 1980, **80**, 231.
5 T. B. Malloy, Jr., L. E. Bauman and L. A. Carreira, *Top Stereochem.*, 1979, **11**, 97; F. G. Riddel, *The Conformational Analysis of Heterocyclic Compounds*, Academic Press, London, 1980, p 1.
6 E. G. Janzen, *Top. Stereochem.*, 1971, **6**, 177.
7 G. Binsch, *Top Stereochem.*, 1968, **3**, 97.
8 J. J. Windle, J. A. Kuhnle and B. H. Beck, *J. Chem. Phys.*, 1969, **50**, 2630; R. E. Rolfe, K. D. Sales and J. H. P. Utley, *J. Chem. Soc., Chem. Commun.*, 1970, 540; *J. Chem. Soc., Perkin Trans. 2*, 1973, 1171; B. C. Gilbert, R. O. C. Norman and M. Trenwith, *J. Chem. Soc., Perkin Trans. 2*, 1974, 1033.
9 (*a*) L. Sjöqvist, A. Lund and J. Maruani, *Chem. Phys.*, 1988, **125**, 293; (*b*) L. Sjöqvist, M. Lindgren and A. Lund, *Chem. Phys. Lett.*, 1989, **156**, 323; (*c*) M. Shiotani, L. Sjöqvist, A. Lund, S. Lunell, L. Eriksson and M. B. Huang, *J. Phys. Chem.*, 1990, **94**, 8081; (*d*) Y. Kubozono, M. Okada, M. Aoyagi, S. Yahiro, H. Nakamura and T. Matsuo, *Z. Naturforsch., Teil A*, 1991, **46**, 993.
10 A. Rockenbauer, M. Győr, H. O. Hankovsky and K. Hideg, *Electron Spin Resonance*, ed. M. C. R. Symons, Royal Society of Chemistry, Cambridge, 1988, vol. 11A, p. 145.
11 E. W. Stone and A. H. Maki, *J. Chem. Phys.*, 1962, **37**, 1326.
12 C. Heller and H. M. McConnell, *J. Chem. Phys.*, 1960, **32**, 1535.
13 D. O. Harris, G. G. Engerholm, C. A. Tolman, A C. Luntz, R. A. Keller, H. Kim and W. D. Gwinn, *J. Chem. Phys.*, 1969, **50**, 2438.
14 H. J. Geise, C. Altona and C. Romers, *Tetrahedron Lett.*, 1967, **15**, 1383; D. Cremer and J. A. Pople, *J. Am. Chem. Soc.*, 1975, **97**, 1354.
15 L. A. Carreira and R. C. Lord, *J. Chem. Phys.*, 1969, **51**, 3225; W. H. Green, A. B. Harvey and J. A. Greenhouse, *J. Chem. Phys.*, 1971, **54**, 850; T. Ikeda and R. C. Lord, *J. Chem. Phys.*, 1972, **56**, 4450.
16 P. J. Krusic and J. K. Kochi, *J. Am. Chem. Soc.*, 1971, **93**, 846.
17 B. Fuchs and P. S. Wechsler, *Tetrahedron*, 1977, **33**, 57.
18 (*a*) S. S. Ament, J. B. Wetherington, J. W. Moncrief, K. Flohr, M. Mochizuki and E. T. Kaiser, *J. Am. Chem. Soc.*, 1973, **95**, 7896; J. B. Wetherington, S. S. Ament and J. W. Moncrief, *Acta Crystallogr., Sect. B*, 1974, **30**, 568; (*b*) B. Chion and J. Lajzerowicz, *Acta Crystallogr., Sect. B.*, 1975, **31**, 1430; (*c*) B. Chion, *Cryst. Struct. Commun.*, 1978, **7**, 395; (*d*) B. Chion, J. Lajzerowicz, A. Collet and J. Jacques, *Acta Crystallogr., Sect. B*, 1976, **32**, 339; (*e*) J. F. Keana, K. Hideg, G. B. Birrell, O. H. Hankovszky, G. Ferguson and M. Parvez, *Can. J. Chem.*, 1982, **60**, 1439.
19 E. L. Eliel and C. A. Giza, *J. Org. Chem.*, 1968, **33**, 3754.
20 Y. Zhang and G. Xu, *J. Chem. Soc., Chem. Commun.*, 1988, 1629; *Magn. Reson. Chem.*, 1989, **27**, 846; *J. Chem. Res. (S)*, 1990, 104.
21 E. G. Janzen, U. M. Oehler, D. L. Haire and Y. Kotake, *J. Am. Chem. Soc.*, 1986, **108**, 6858; D. L. Haire, Y. Kotake and E. G. Janzen, *Can. J. Chem.*, 1988, **66**, 1901.
22 J. A. Dale, D. L. Dull and H. S. Mosher, *J. Org. Chem.*, 1969, **34**, 2543.
23 E. G. Rozantsev, *Free Nitroxyl Radicals*, Plenum, New York, 1970, p. 217.
24 K. Hideg, H. O. Hankovszky, L. Lex and Gy. Kulcsár, *Synthesis*, 1980, 911.
25 H. O. Hankovszky, K. Hideg, L. Lex, Gy. Kulcsár and H. A. Halász, *Can. J. Chem.*, 1982, **60**, 1432.
26 K. Hideg, H. O. Hankovszky and H. A. Halász, *J. Chem. Soc., Perkin Trans. 1*, 1988, 2905.
27 K. Hideg, unpublished results.
28 H. O. Hankovszky, K. Hideg, Gy. Jerkovich, A. Rockenbauer, M. Győr and P. Sohár, *Can. J. Chem.*, 1989, **67**, 1392.
29 K. Hideg and L. Lex, *J. Chem. Soc., Chem. Commun.*, 1984, 1263.

Paper 3/01327H
Received 8*th March* 1993
Accepted 10*th August* 1993